Evolution of Raman spectra as a function of layer thickness in ultra-thin InSe films

2002 J. Phys.: Condens. Matter 14 967

(http://iopscience.iop.org/0953-8984/14/5/302)

INSTITUTE OF PHYSICS PUBLISHING JOURNAL OF PHYSICS: CONDENSED MATTER

J. Phys.: Condens. Matter **14** (2002) 967–973 PII: S0953-8984(02)27940-0

Evolution of Raman spectra as a function of layer thickness in ultra-thin InSe films

R Schwarcz[1], M A Kanehisa[1], M Jouanne[1], J F Morhange[1] and M Eddrief[2]

[1] Laboratoire des Milieux Désordonnés et Hétérogènes UMR 7603, Université Pierre et Marie Curie, Tour 22, 4, Place Jussieu, 75252 Paris Cédex 05, France
[2] Laboratoire de Minéralogie–Cristallographie UMR 7590, Universités Pierre et Marie Curie et D Diderot, Tour 16, 4, Place Jussieu, 75252 Paris Cédex 05, France

E-mail: res@ccr.jussieu.fr

Received 16 August 2001, in final form 7 January 2002
Published 25 January 2002
Online at stacks.iop.org/JPhysCM/14/967

Abstract

Experimentally, when compared with III–V, II–VI, or IV–IV layered systems, the InSe Raman spectrum does not change very much as a function of the number of InSe layers. A simple linear chain model is sufficient to explain this effect. In our model, two parameters are used to characterize Raman spectra: the halfwidth Γ characterizing the sample quality and the coherence length Λ determined by the sample thickness n. Our analysis shows that the coherence length Λ is linear in n. We obtain a fair agreement between computed and experimental Raman spectra.

1. Introduction

During the last few years, a new technique called 'van der Waals' epitaxy has been developed for the growth of heterostructures using layer-type semiconductors [1–7]. Molecular beam epitaxy (MBE) is used to growth ultra-thin films whose thickness can be as small as a few atomic layers. Such ultra-thin films have recently been studied extensively by various methods such as the reflection high-energy electron diffraction (RHEED) [8], x-ray diffraction [5], and x-ray standing-wave diffraction techniques [6]. Another very useful technique for controlling the quality of these thin films is Raman scattering. Raman spectroscopy has been frequently used to study conventional superlattices based on III–V compounds [9–11], II–VI materials [8,12–14], and IV–IV systems [15] (see [16] for a review). Recently, it was also applied to weak Raman signals from extremely thin films and to characterize their structural properties [7, 10, 11, 17]. Thus it is interesting to theoretically study the vibrational properties of thin van der Waals epitaxial layers [18] and compare them with the results of Raman scattering experiments.

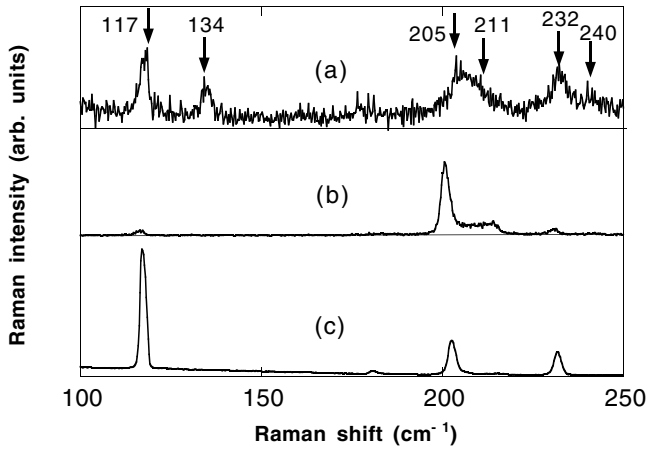

Figure 1. Raman spectra of thin InSe films on GaSe/Si. Sample thickness n (in layers): (a) $n = 3$ and (b) $n = 21$; (c) bulk.

In this paper, we make a direct comparison between theoretical (computed) and experimental Raman spectra of InSe films grown on GaSe substrates and we study their evolution as a function of the layer thickness.

2. Experiment

MBE growth techniques are used to prepare ultra-thin films of a few atomic layers of InSe on a buffered GaSe/Si(111) substrate [19]. A layer has to be understood as an elemental sheet constituted of an Se–In–In–Se atomic plane sequence, with a thickness of 8.32 Å [20]. The weakness of the interlayer coupling between two layered materials like InSe and GaSe can counterbalance a large lattice mismatch (6.7%) between the first epitaxial layers and the substrate. Thus, almost relaxed InSe films can be produced with the same lattice constants as the bulk [21]. Growth of InSe and GaSe films was carried out in the same MBE chamber with a base pressure better than 10^{-10} Torr. RHEED was used to monitor the quality of the silicon substrate surface and the structure of the films during epitaxial growth. More details about growth conditions and characterization techniques for GaSe and InSe can be found elsewhere [19, 22].

Raman spectra were measured at low temperatures using a double-grating monochromator. The 488 nm line of an Ar^+ laser was focused on the sample along its c-axis in a quasi-back-scattering geometry. At low temperature, this photon energy is resonant with the second exciton of InSe situated at the gap E_1' between the p_x–p_y-like valence band and the s-like conduction band [23, 24]. The power density was 250 W cm^{-2}.

Raman spectra are presented in figure 1. The three spectra correspond respectively to InSe samples consisting of 3 layers (figure 1(a)) and 21 layers (figure 1(b)), and a bulk InSe sample (figure 1(c)). The two thin layered samples were deposited on silicon substrates covered with a buffer layer of GaSe.

When the number n of InSe layers stacked along the c-axis of the GaSe epilayer is small, the Raman spectrum presents broad bands (FWHM $=$ 10 cm^{-1}) as shown in figure 1(a). With increasing n, the InSe bands become narrower, as illustrated in figures 1(b) and (c).

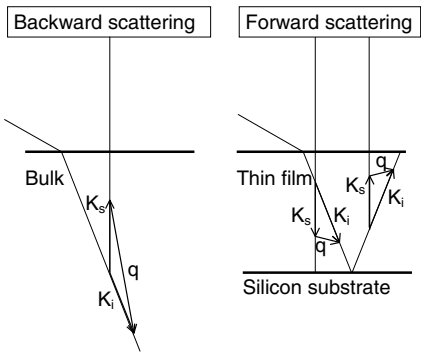

Figure 2. Mechanism of observation of the forbidden in-plane wavevector phonon in thin films.

The bands observed at 117, 205, and 232 cm^{-1} correspond respectively to the Γ_1^2, Γ_1^1, and Γ_1^3 phonons of InSe. The bands at 134, 240, and 311 cm^{-1} (this last band is not shown in the figure) can be attributed to the phonon modes of the GaSe buffer with the same symmetry as those in the InSe layers. The GaSe bands are hardly observable for the thicker layer of InSe (figure 1(b)) because of its optical absorption. The peak observed at 211 cm^{-1} (figures 1(b) and (c)) appears more intense in thin films of 21 layers than in bulk. This peak is due to scattering by a LO phonon of InSe polarized along the layer plane and is forbidden in a back-scattering configuration when the wavevector is normal to the layer plane. Due to its reflection on the substrate, the forward-scattered Raman component can be detected together with the backwards-scattered component, which makes possible the observation of phonons with a wavevector parallel to the layer plane, as illustrated in figure 2.

Experimentally, the InSe Raman spectrum is almost independent of the number n of InSe layers. This result is completely different from those found for III–V [9–11], II–VI [8, 12–14], or IV–IV [15] layered systems, where series of n LO peaks are observed for films of n layers. These compounds, with zinc-blende or diamond structure, are 3D crystals, and the atomic planes are strongly bonded by semi-ionic or covalent bonds. In the case of InSe, the bulk is constituted of In_2Se_2 layers weakly bound by van der Waals forces. For this reason, the vibration coherence length along the c-axis is small (a few layers). Consequently, confinement effects may appear significantly for thickness smaller than the coherence length of bulk vibrations. Experimentally, we begin to observe spectral changes of Raman bands due to spatial correlated effects for thickness of about three layers (In_2Se_2). A model which reproduces the experimental Raman spectra, introducing the coherence length as a parameter, is presented in the next section.

3. Model

Let us first consider bulk GaSe and InSe. These are III–VI group semiconductors and have identical layered structure, each layer consisting of two single planes of Se atoms on both sides of two planes of metal atoms (Ga or In) stacked along the c-axis. Since we are interested in the effect of heterostructure formation along the c-axis, we use a linear chain model with nearest-neighbour short-range interactions for lattice dynamics [9, 25]. For bulk InSe, the dispersion curve as a function of k_z obtained in this way is shown in figure 3, where c is the lattice constant along the c-axis.

Next we consider thin films consisting of n layers of InSe stacked on a single-layer GaSe substrate. In this case, we need interlayer force constants between heterogeneous layers.

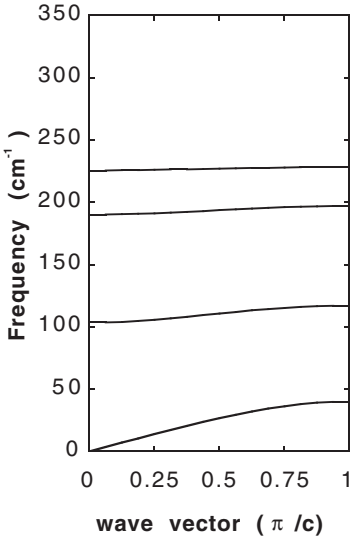

Figure 3. The calculated phonon dispersion curve along the *c*-axis in InSe (longitudinal modes).

We use averages of two corresponding bulk values [26]. In thin films, each layer contains four atoms. Thus for a one-layer GaSe substrate and n layers of InSe, we have to solve $4(n+1)$ secular equations. By diagonalizing the corresponding dynamical matrices, we obtain the normal-mode frequencies and associated eigenvectors giving the atomic displacements in different layers. The result for n up to 20 is shown in figure 4. The modes at 307, 237, and 122 cm^{-1} are substrate (GaSe) modes and do not depend on n. All the other modes vary with n. Atomic displacement study shows that the optical modes (232, 205, and 117 cm^{-1}) are mostly confined in the InSe layers while the acoustic modes ($<$50 cm^{-1}) are spatially delocalized. From figure 4, we obtain that for the values of the layer thickness that we are interested in, the spectra cover most of the possible frequency ranges expected from the dispersion curve (figure 3) and that the energy levels are closely spaced due to the small dispersion of the optical branches. It should be also noted that it is not possible to include the wavevector selection rule in this type of calculation without making further assumptions. Thus it is meaningful to start from the bulk material and incorporate the finiteness of the sample. This is done as follows.

The intensity of Raman scattering where incident light $\vec{k}_i$ is scattered into $\vec{k}_s$ is given by

$$I(\omega) = \sum_{\vec{k}s} f_{\vec{q}}(\vec{k}, s) A_{\vec{k}s}(\omega). \tag{1}$$

Here $\vec{q} = \vec{k}_i - \vec{k}_s$ is the wavevector transfer. The factor $f_{\vec{q}}(\vec{k}, s)$ is the scattering function describing the coupling between the light and the phonon of wavevector $\vec{k}$ in the branch s. $A_{\vec{k}s}(\omega)$ is the spectral function for the mode $\vec{k}s$ and $\omega_s(\vec{k})$ is the phonon dispersion relation:

$$A_{\vec{k}s}(\omega) = \delta(\omega - \omega_s(\vec{k})). \tag{2}$$

Under the assumption of a finite damping rate Γ due to the spectral width and sample imperfections, and taking in account anharmonicity effects, we consider equation (3) instead of equation (2):

$$A_{\vec{k}s}(\omega) = \frac{\Gamma/\pi}{(\omega - \omega_s(\vec{k}))^2 + \Gamma^2}. \tag{3}$$

This is a Lorentzian with width Γ. Equation (3) is reduced to equation (2) for $\Gamma \to 0$.

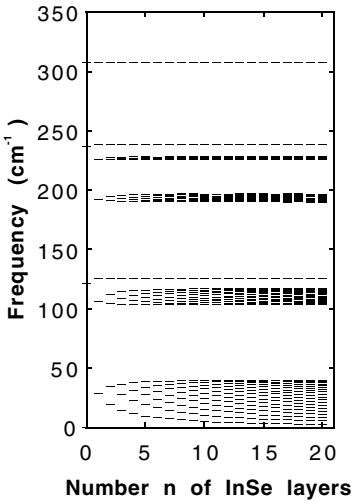

Figure 4. Variations of normal-mode frequencies of thin InSe films as a function of the number of layers n.

We consider now the scattering function $f_{\vec{q}}(\vec{k}, s)$ in (1): for perfect crystals, the wavevector conservation rule during the scattering process implies

$$f_{\vec{q}}(\vec{k}, s) \propto \delta_{\vec{k}\vec{q}} = \delta_{k_x q_x} \delta_{k_y q_y} \delta_{k_z q_z}. \tag{4}$$

For amorphous materials, $f_{\vec{q}}(\vec{k}, s)$ is independent of $\vec{k}$:

$$f_{\vec{q}}(\vec{k}, s) = 1 \tag{5}$$

and the Raman scattering intensity in equation (1) reflects essentially the density of states [27, 28]. For partially disordered materials, one may consider a state intermediate between the crystalline (equation (1)) and the amorphous (equation (5)) states in the form

$$f_{\vec{q}}(\vec{k}, s) \propto \mathrm{e}^{-(\vec{k}-\vec{q})^2 \Lambda^2} \tag{6}$$

where Λ is a measure of the coherence length. For large and small Λ^{-1}, equation (6) naturally reduces to (4) and (5), respectively. Thin films conserve the translational symmetry in the layer (x, y) but not along z. Therefore, one may use a mixture of equations (4) and (6) in the form

$$f_{\vec{q}}(\vec{k}, s) \propto \delta_{k_x q_x} \delta_{k_y q_y} \mathrm{e}^{-(k_z - q_z)^2 \Lambda^2}.$$

We expect the coherence length Λ here to increase with the film thickness n. Campbell and Fauchet [29] took a similar approach using Gaussian functions for calculating line shapes in various confined structures. In the case of thin films, their spectral function (equation (11) of their paper) is essentially our equation (6) multiplied by a corrective factor due to a cut-off effect.

We shall now calculate the Raman intensity according to equation (1) and compare it with the intensities of the Raman spectra of figure 1. Numerical integration of equation (1) is straightforward for finite values of Γ. When $\Gamma = 0$ the integral involves the delta function (equation (2)), and can be calculated by the Gilat–Raubenheimer method [30] adapted to one dimension. From the experimental values of figure 1(c), the halfwidth at half-maximum Γ is about 1 cm^{-1}. We calculate the Raman intensity (equation (1)) for different values of the coherence length Λ and, for each value of n, we choose the value of Λ which allows the best

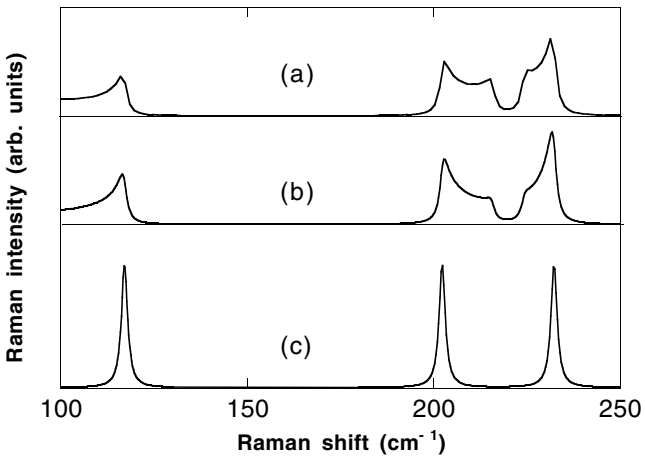

Figure 5. Theoretical Raman spectra of thin InSe films for various thickness n: (a) $n = 3$ and (b) $n = 21$; and (c) bulk.

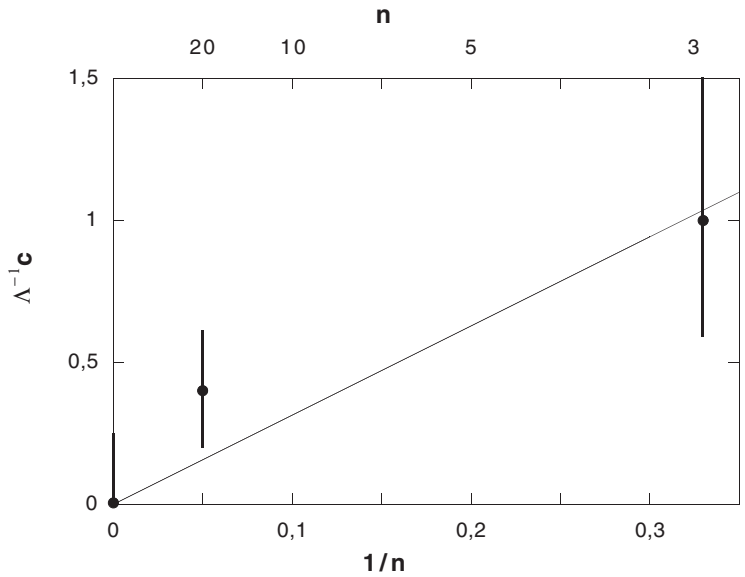

Figure 6. The inverse coherence length Λ^{-1} (times c) as a function of $1/n$. The straight line represents $\Lambda^{-1}c = \pi/n$.

reproduction of the positions and widths of the Raman bands. The result is shown in figure 5 and is compared with the experimental spectra of figure 1. The agreement in band positions seems reasonable and the general tendency is correctly reproduced. (The experimental noise in figure 1(a) is due to the extremely weak Raman signal from a very thin sample.)

In figure 6, we plot $\Lambda^{-1}c$ as a function of the inverse thickness $1/n$. Here $n = \infty$ corresponds to the bulk. The error bar represents the acceptable parameter range for a given value of $1/n$. The plot shows that Λ^{-1} and $1/n$ are linearly related, as expected. The straight line represents $\Lambda^{-1}c = \pi/n$, which is theoretically expected. Though there are only three experimental points with large error bars, the agreement may be considered as fair and we may consider our model as reasonable.

4. Conclusions

We studied, both experimentally and theoretically, the evolution of Raman spectra as a function of layer thickness in InSe thin films. We calculated the Raman spectra numerically, taking into account the finite thickness of the samples. Two parameters were used to characterize Raman spectra: the halfwidth Γ and the coherence length Λ. We obtain a fair agreement between theoretically predicted and experimentally determined Raman bands. Our analysis shows that the coherence length Λ is linear in n, as expected.

References

[1] Koma A and Yoshimura K 1986 *Surf. Sci.* **174** 556
[2] Ueno K, Shimada T, Saiki K and Koma A 1990 *Appl. Phys. Lett.* **4** 327
[3] Lang O, Schlef R, Tomm Y, Pettenkofer C and Jaegermann W 1994 *J. Appl. Phys.* **75** 7805
[4] Vinh L T, Eddrief M, Mahan J E, Vantomme A, Song J H and Nicolet M A 1997 *J. Appl. Phys.* **81** 7289
[5] Jedrecy N, Pinchaux R and Eddrief M 1997 *Phys. Rev.* B **56** 9583
[6] Koebel A, Zheng Y, Petroff J F, Boulliard J C, Capelle B and Eddrief M 1997 *Phys. Rev.* B **56** 12 296
[7] Morhange J F, Jouanne M, Sacuto A, Le Thanh V, Eddrief M, Kanehisa M A, Ivanov I and Schwarcz R 1994 *The Physics of Semiconductors* (Singapore: World Scientific) p 297
[8] Hetterich M, Grun M, Petri W, Markle C, Klingshirn C, Wurl A, Fischer U, Rosenauer A and Gerthsen D 1997 *Phys. Rev.* B **56** 12 369
[9] Colvard C, Gant T A, Klein M V, Merlin R, Fischer R, Morkoc H and Gossard A C 1985 *Phys. Rev.* B **31** 2080
[10] Tran C A, Brebner J L, Leonelli R, Jouanne M and Masut R A 1994a *Phys. Rev.* B **49** 11 268
[11] Tran C A, Brebner J L, Leonelli R, Jouanne M and Masut R A 1994b *Superlatt. Microstruct.* **15** 391
[12] Nakashima H, Nakakura Y, Fujiyasu H and Mochizuki K 1986 *Appl. Phys. Lett.* **48** 236
[13] Fromherz T, Eunsoon O H, Ramdas A K, Koppensteiner E, Bauer G, Faschinger W and Sitter H 1994 *J. Cryst. Growth* **138** 580
[14] Yamamoto A, Kanemitsu Y and Masumoto Y 1994 *J. Cryst. Growth* **138** 643
[15] Kumar S and Trodahl Masumoto H J 1991 *J. Appl. Phys.* **70** 508
[16] Jusserand B and Cardona M 1989 *Springer Topics in Applied Physics* vol 66 (Berlin: Springer) p 49
[17] Quagliano L G, Jusserand B and Orani D 1996 *Solid-State Electron.* **40** 711
[18] Schwarcz R and Kanehisa M A 1996 *5èmes Journées de la Matière Condensée Organisées par la Société Française de Physique (Orléans)* unpublished
[19] Le Thanh V, Eddrief M, Sebenne C A, Sacuto A and Balkanski M 1994 *J. Cryst. Growth* **135** 1
[20] Rigoult J, Rimsky A and Kuhn A 1980 *Acta Crystallogr.* B **36** 916
[21] Emery J Y *et al* 1992 *J. Appl. Phys.* **71** 3256
[22] Brahim-Otsmane L, Emery J Y and Eddrief M 1994 *Thin Solid Films* **237** 291
[23] Kuroda N and Nishina Y 1978 *Solid State Commun.* **28** 439
[24] Piccioli N, Le Toullec R, Bertrand F and Chervin J C 1981 *J. Physique* **42** 1129
[25] Wieting T J 1973 *Solid State Commun.* **12** 931
[26] Schwarcz R and Kanehisa M A 1994 *Solid State Commun.* **8** 689
[27] Shuker R and Gammon R W 1970 *Phys. Rev. Lett.* **25** 222
[28] Shuker R and Gammon R W 1971 *Proc. 2nd Int. Conf. on Light Scattering in Solids* (Paris: Flammarion Sciences) p 334
[29] Campbell I H and Fauchet P M 1986 *Solid State Commun.* **58** 739
[30] Gilat G and Raubenheimer L J 1966 *Phys. Rev.* **144** 390